Electronic Supplementary Material (ESI) for RSC Advances.

Supporting Information

Synergistic catalytic effects of oxygen and nitrogen functional groups on active carbon electrodes for all-vanadium redox flow batteries

Min Eui Lee,[a] Hyoung-Joon Jin,[*a] and Young Soo Yun[*b]

[a]*WCSL(World Class Smart Lab) of Green Battery Lab., Department of Polymer Science and Engineering, Inha University, 100, Inha-ro, Nam-gu, Incheon 22201, South Korea*

[b]*Department of Chemical Engineering, Kangwon National University, 346, Jungang-ro, Samcheok-si, Gangwon-do 25913, South Korea*

[*]These authors contributed equally to this work.

[*] E-mail: hjjin@inha.ac.kr and ysyun@kangwon.ac.kr

Table S1. Surface properties of CFs and P-CFs prepared with different heat-treatment temperatures.

Atomic ratio	Sample					
	CFs	P-CFs-400	P-CFs-600	P-CFs-800	P-CFs-1000	P-CFs-1200
C/O	15.8	8.6	13.6	15.7	17.3	20.8
C/N	84.5	12.1	17.7	30.4	32.8	52.1

Table S2. Surface properties of CFs and O-CFs prepared with different heat-treatment temperatures.

Atomic ratio	Sample					
	CFs	O-CFs-400	O-CFs-600	O-CFs-800	O-CFs-1000	O-CFs-1200
C/O	15.8	4.5	8.7	10.5	11.3	15.0

Table S3. Surface properties of CFs and N-CFs prepared with different heat-treatment temperatures.

Atomic ratio	Sample					
	CFs	N-CFs-400	N-CFs-600	N-CFs-800	N-CFs-1000	N-CFs-1200
C/N	84.5	7.5	12.1	13.7	22.0	34.2

Table S4. Electrochemical performance from cyclic voltammograms for CFs and O-CFs acquired at a sweep rate of 5 mV s^{-1}.

electrode	Anode						Cathode					
	I_{pa} (mA)	I_{pc} (mA)	V_{pa} (V)	V_{pc} (V)	I_{pa}/I_{pc}	ΔE_p (mV)	I_{pa} (mA)	I_{pc} (mA)	V_{pa} (V)	V_{pc} (V)	I_{pa}/I_{pc}	ΔE_p (mV)
CFs	50.40	-57.60	-0.39	-0.58	0.86	363.0	39.52	-33.86	1.10	0.66	1.17	435.9
O-CFs-400	64.26	-69.36	-0.31	-0.64	0.93	323.4	59.58	-47.12	1.13	0.84	1.26	287.9
O-CFs-600	67.30	-73.06	-0.32	-0.65	0.92	336.9	57.91	-48.47	1.16	0.85	1.03	315.0
O-CFs-800	62.04	-68.33	-0.31	-0.65	0.91	345.2	61.87	-59.89	1.16	0.84	1.19	322.9
O-CFs-1000	64.69	-67.50	-0.30	-0.65	0.96	353.0	60.53	-50.84	1.17	0.84	1.17	331.0
O-CFs-1200	64.08	-70.43	-0.29	-0.65	0.91	359.1	67.65	-57.64	1.17	0.82	1.19	342.9

Table S5. Electrochemical performance from cyclic voltammograms of CFs and N-CFs acquired at a sweep rate of 5 mV s^{-1}.

electrode	Anode						Cathode					
	I_{pa} (mA)	I_{pc} (mA)	V_{pa} (V)	V_{pc} (V)	I_{pa}/I_{pc}	ΔE_p (mV)	I_{pa} (mA)	I_{pc} (mA)	V_{pa} (V)	V_{pc} (V)	I_{pa}/I_{pc}	ΔE_p (mV)
CFs	50.40	-57.60	-0.39	-0.58	0.86	363.0	39.52	-33.86	1.10	0.66	1.17	435.9
N-CFs-400	65.72	-79.53	-0.37	-0.61	0.83	238.0	72.06	-64.93	1.01	0.72	1.11	290.1
N-CFs-600	78.37	-87.30	-0.36	-0.66	0.90	291.8	73.88	-68.01	1.06	0.75	1.09	352.4
N-CFs-800	74.74	-81.12	-0.37	-0.68	0.92	311.5	83.72	-71.33	1.12	0.75	1.17	366.1
N-CFs-1000	76.98	-84.69	-0.32	-0.65	0.91	327.3	74.13	-67.24	1.07	0.74	1.10	375.3
N-CFs-1200	70.66	-76.79	-0.33	-0.68	0.92	352.4	79.59	-69.19	1.12	0.73	1.15	385.2

Table S6. Electrochemical performance from cyclic voltammograms of CFs and P-CFs acquired at a sweep rate of 5 mV s^{-1}.

electrode	Anode						Cathode					
	I_{pa} (mA)	I_{pc} (mA)	V_{pa} (V)	V_{pc} (V)	I_{pa}/I_{pc}	ΔE_p (mV)	I_{pa} (mA)	I_{pc} (mA)	V_{pa} (V)	V_{pc} (V)	I_{pa}/I_{pc}	ΔE_p (mV)
CFs	50.40	-57.60	-0.39	-0.58	0.86	363.0	39.52	-33.86	1.10	0.66	1.17	435.9
P-CFs-400	77.95	-81.27	-0.40	-0.57	0.97	170.9	71.89	-66.18	1.02	0.72	1.10	302.0
P-CFs-600	65.87	-73.72	-0.40	-0.59	0.89	190.4	65.31	-58.57	1.06	0.68	1.11	371.4
P-CFs-800	51.62	-53.98	-0.35	-0.62	0.96	278.3	58.52	-56.58	1.08	0.68	1.03	395.4
P-CFs-1000	60.36	-67.81	-0.32	-0.66	0.89	341.7	58.47	-54.18	1.10	0.67	1.08	425.2
P-CFs-1200	63.16	-70.15	-0.31	-0.68	0.90	371.1	67.04	-55.41	1.09	0.67	1.21	420.2

Table S7. Summary of electrochemical performances of several heteroatom-doped carbon-based electrodes.

Sample	Based materials	Doped heteroatom	Electrolyte in CV (reference electrode)	Scan rate (mV s^{-1})	ΔE_p (mV)	Ref.
P-CFs	CF*	O and N	0.1 M $VOSO_4$ + 2 M H_2SO_4 (V vs. Ag/AgCl)	1	75	Our work
				5	170	
N-CB-CF	CF	O and N	0.1 M $VOSO_4$ + 3 M H_2SO_4 (V vs. Ag/AgCl)	5	500	19
OGF	GF*	O	0.1 M $VOSO_4$ + 2 M H_2SO_4 (V vs. Ag/AgCl)	5	230	26
NCS/GF	GF	N	0.1 M $VOSO_4$ + 2 M H_2SO_4 (V vs. SCE)	1	142	37

*CF : carbon felt, GF : graphite felt

Table S8. Electrochemical performances of several RFB full cell devices including P-CFs//CFs.

Cell type	Surface modification	Electrode materials	Full-cell		Ref.
			Current density ($mA\ cm^{-2}$)	Energy efficiency (%)	
Flow cell	-	CFs//CFs	100	~45	This work
	Heteroatom doping (Only anode)	P-CFs-400//CFs	100	~66	
	Thermal treatment (Anode and cathode)	TGF//TGF	120	~75	46
		TGF//TGF	100	~81	47

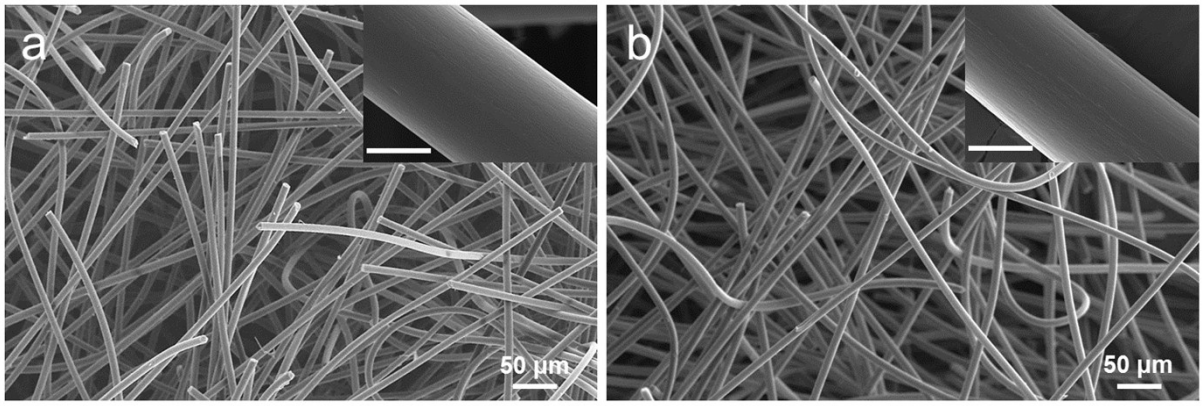

Figure S1. FE-SEM images of (a) N-CFs-400 and (b) O-CFs-400 (Inset: high magnification of FE-SEM images, scale bar: 5 μm).

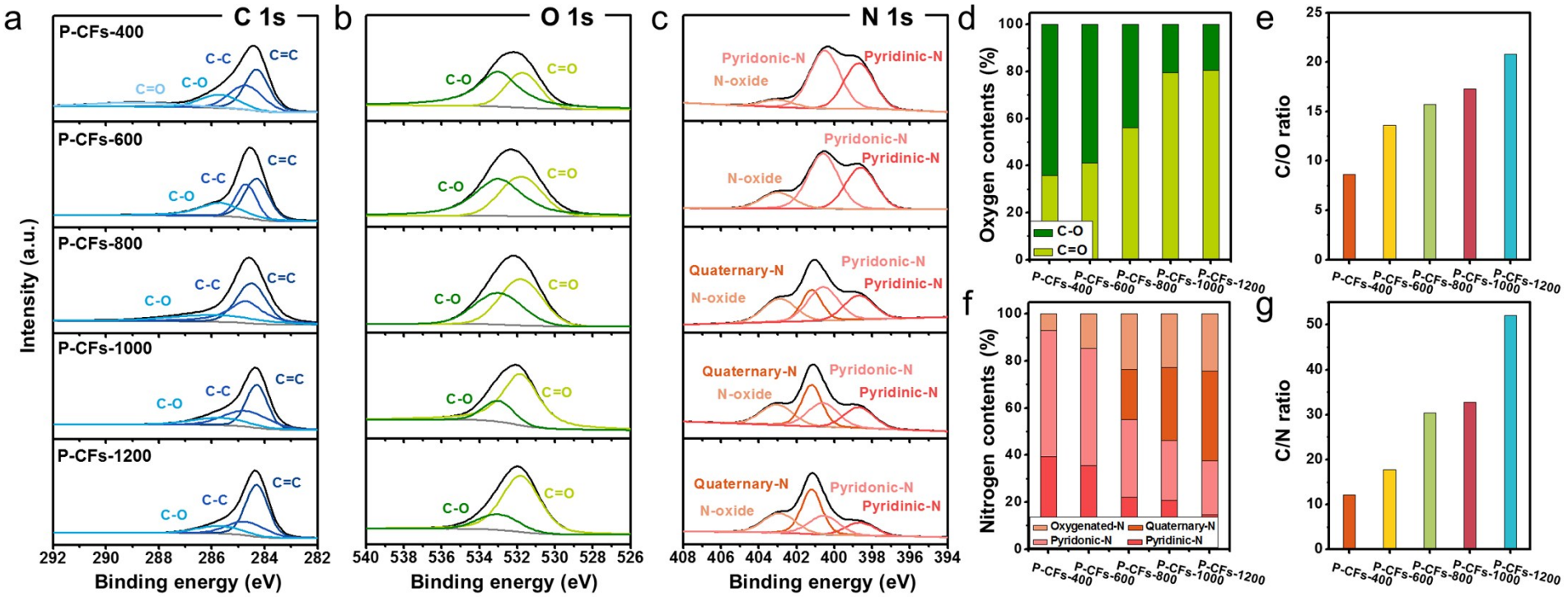

Figure S2. XPS analysis of P-CFs prepared at different heat-treatment temperatures. High-resolution (a) C 1*s*, (b) O 1*s*, and (c) N 1*s* spectra. (d) Oxygen chemical composition and (e) content of oxygen functional groups and (f) nitrogen chemical composition and (g) content of nitrogen functional groups.

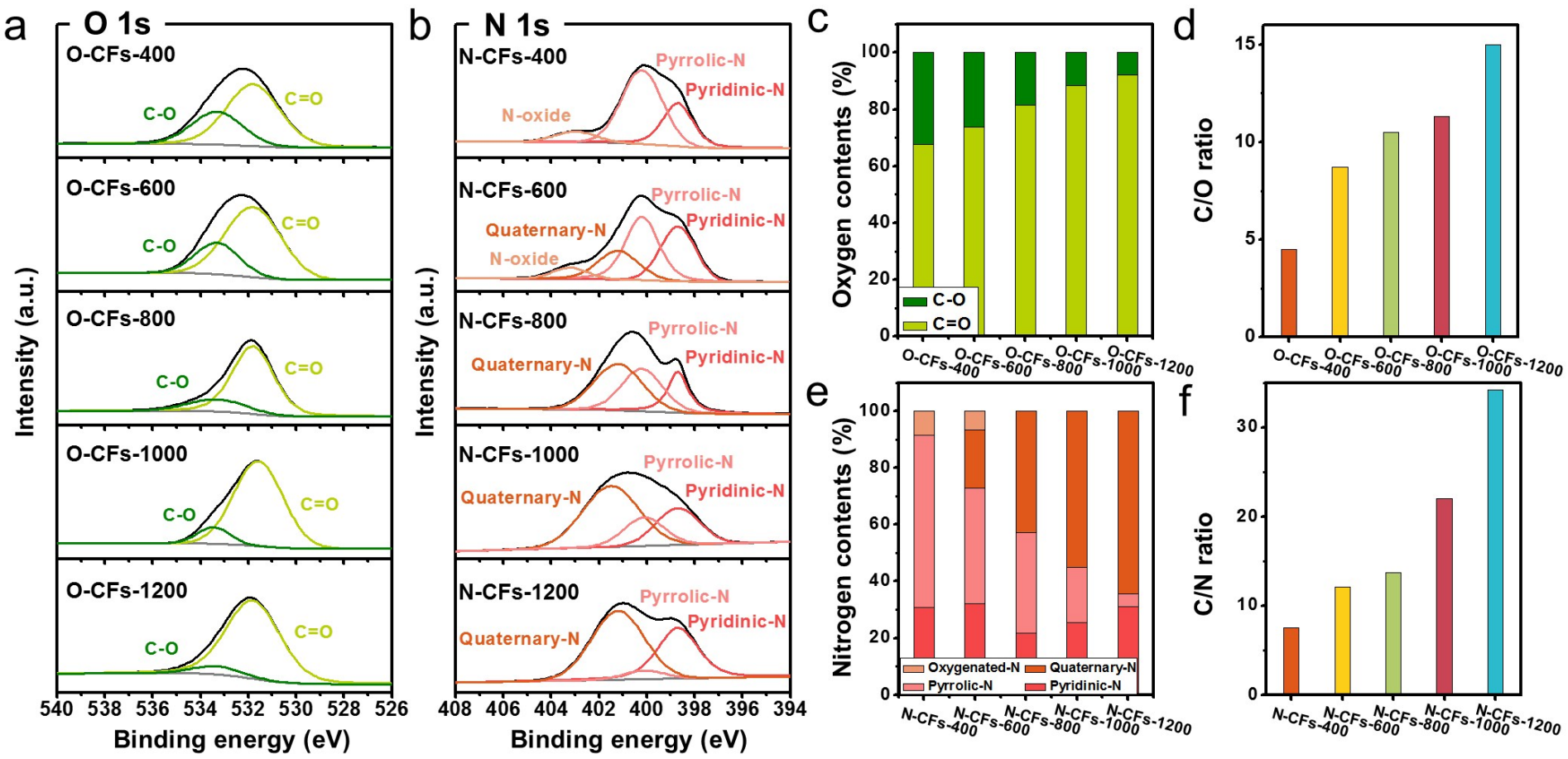

Figure S3. XPS analysis of O-CFs and N-CFs prepared at different heat-treatment temperatures. High-resolution (a) O 1*s* spectra of O-CFs and (b) N 1*s* spectra of N-CFs. (c) Oxygen chemical composition and (d) content of oxygen functional groups of O-CFs and (e) nitrogen chemical composition and (f) content of nitrogen functional groups of N-CFs.

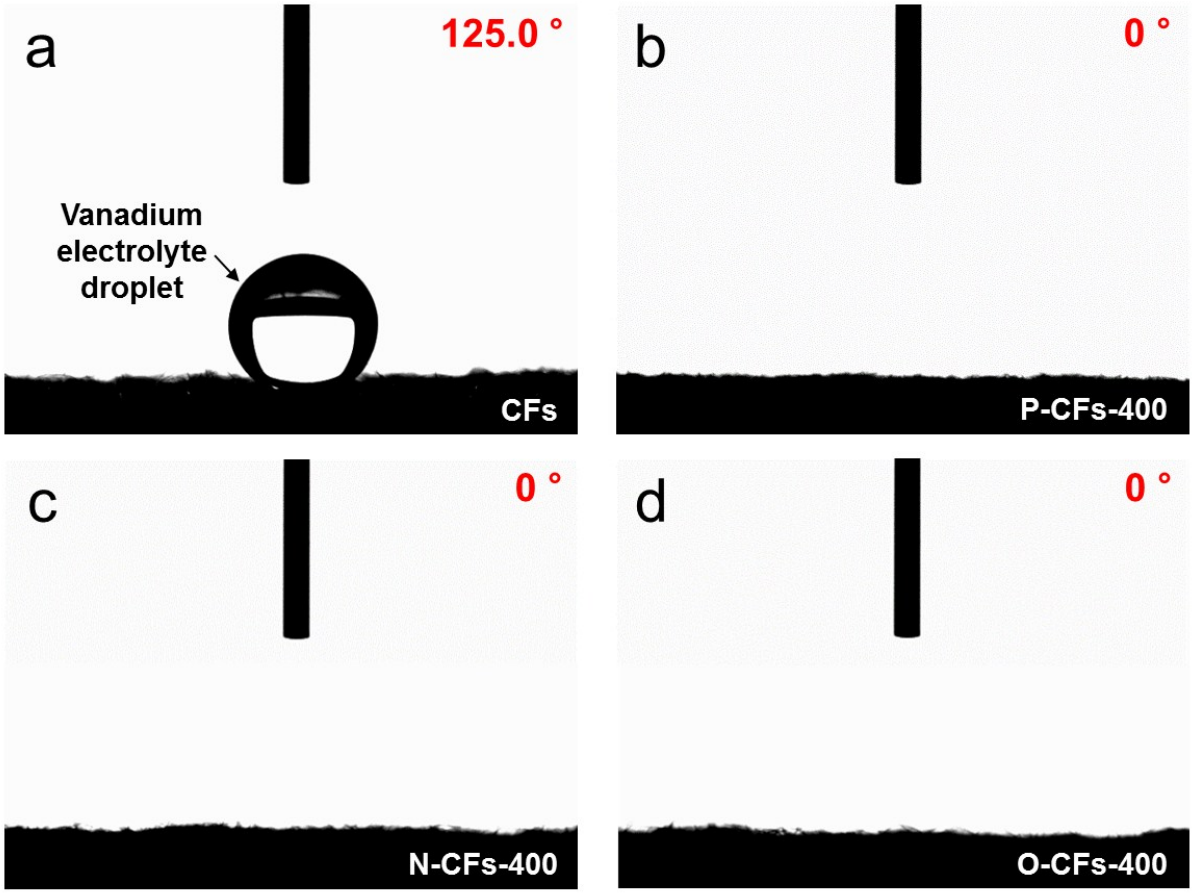

Figure S4. Optical images of contact angle measurement using 0.1 M $VOSO_4$ dissolved in 2 M H_2SO_4 electrolyte on (a) CFs, (b) P-CFs-400, (c) N-CFs-400, and (d) O-CFs-400.

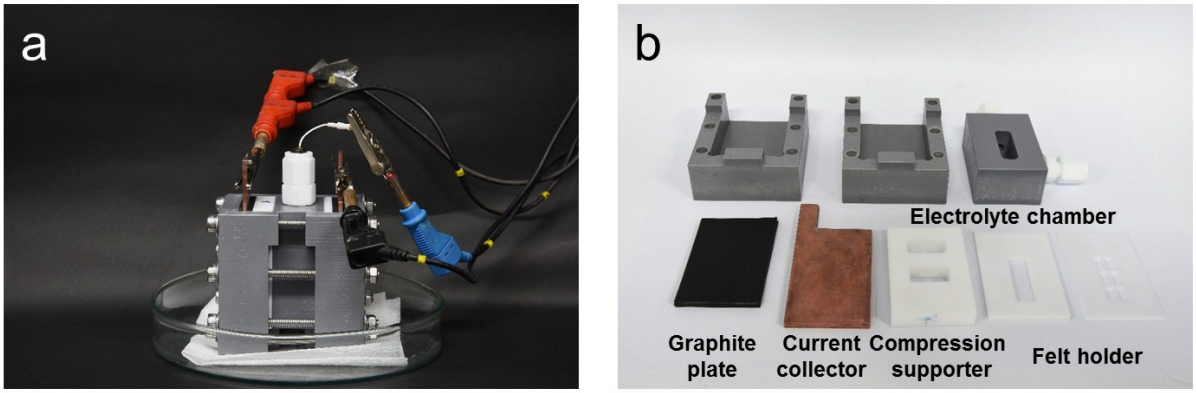

Figure S5. (a) Digital photograph of a hand-made three-electrode configuration system and (b) its components.

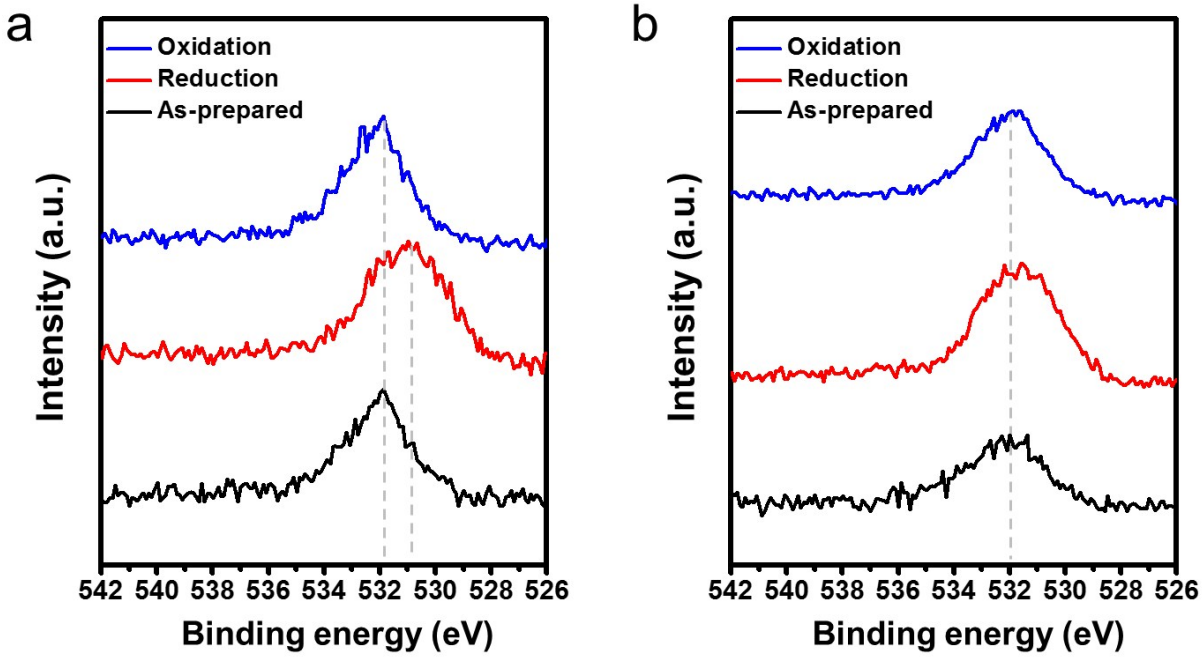

Figure S6. Ex-situ O 1*s* spectra of (a) P-CFs-400 and (b) O-CFs-400 at different states of charge (0, 0.8, and 0 V vs. Ag/AgCl for black, red, and blue, respectively).

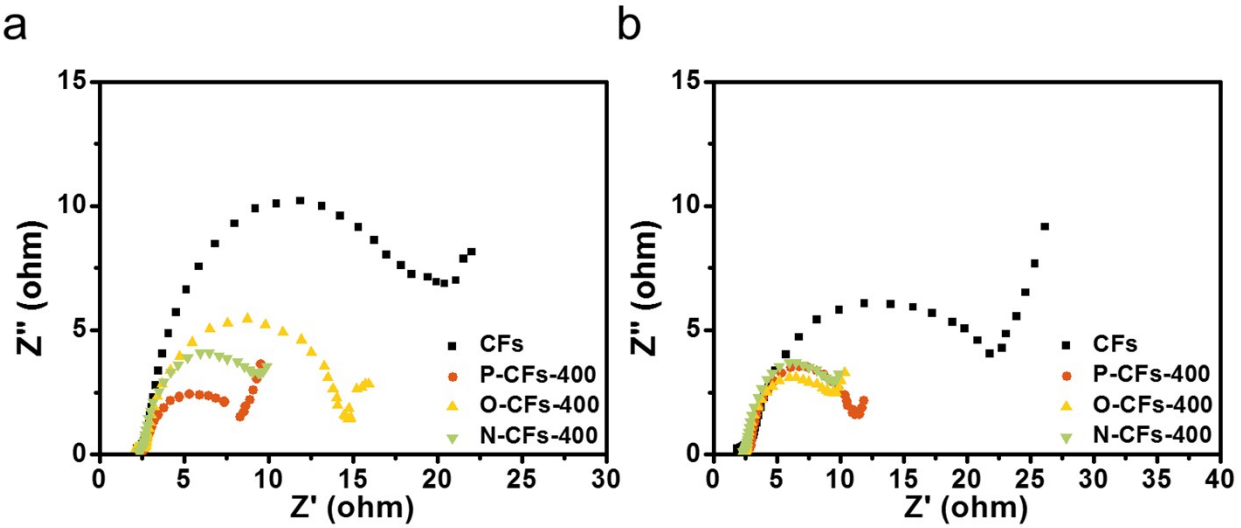

Figure S7. Nyquist plots of CFs, P-CFs-400, O-CFs-400 and N-CFs-400 in (a) anolyte and (b) catholyte.

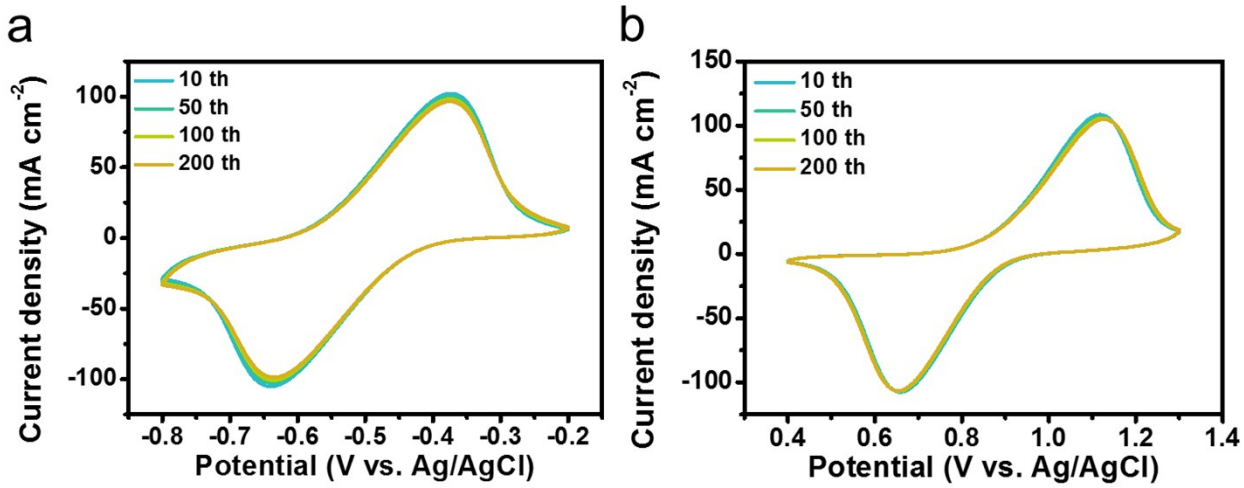

Figure S8. Cyclic stability of P-CFs-400 in (a) anolyte and (b) catholyte. (Scan rate : 10 mV s^{-1})

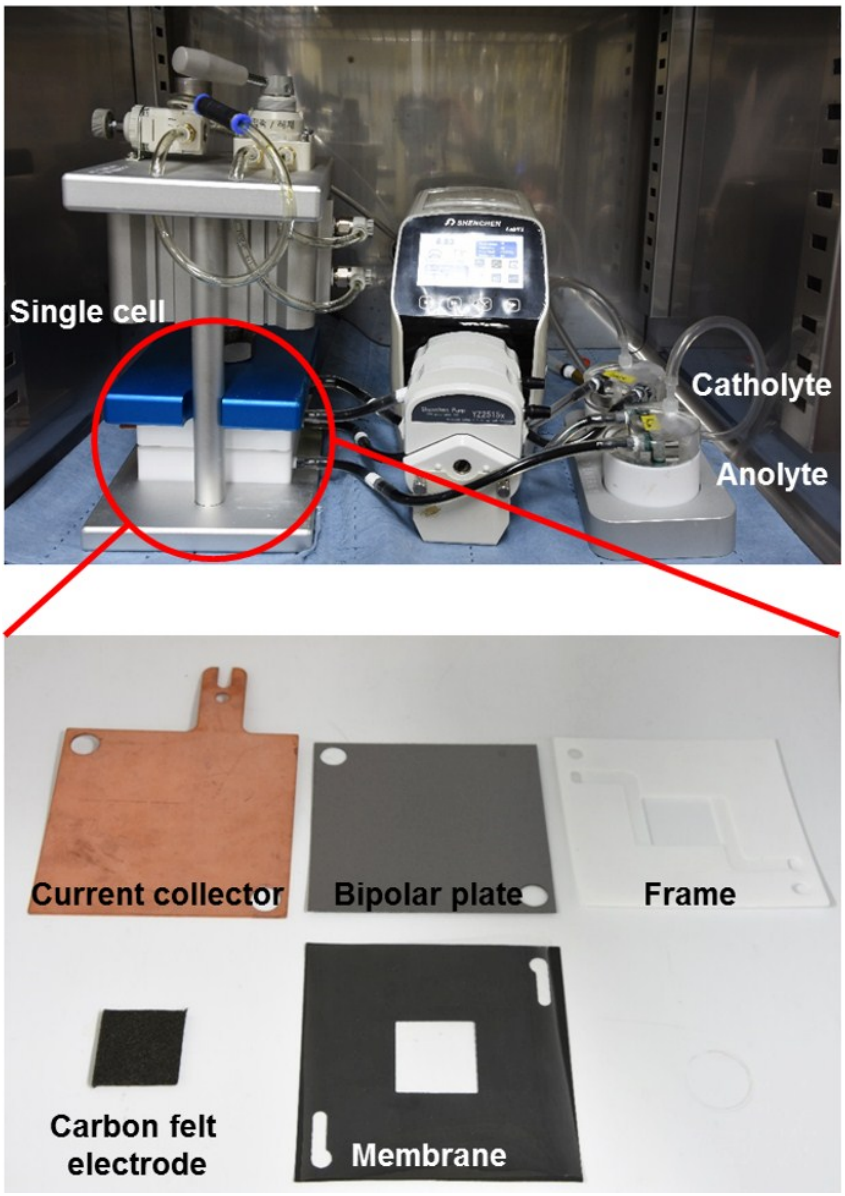

Figure S9. Digital photograph of full-cell VRFB systems comprising a single flow cell composed of current collector, bipolar plate, frame, electrode, and membrane.

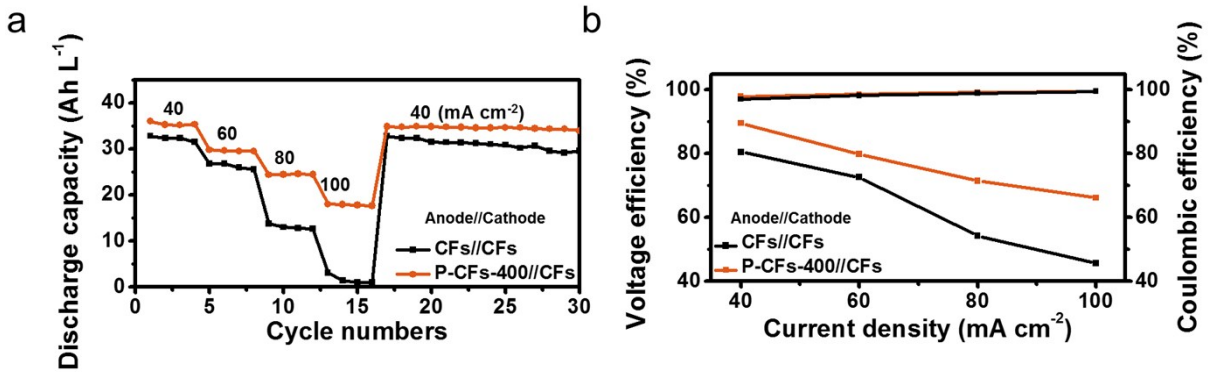

Figure S10. (a) Rate performance at current densities from 40 to 100 mA cm^{-2} and (b) voltage efficiencies and Coulombic efficiencies as a function of cycle number at different current densities for operation of VRFB single-cell based on CFs//CFs and P-CFs-400//CFs.